ADVANCING EARTH AND SPACE SCIENCE

Journal of Geophysical Research: Earth Surface

RESEARCH ARTICLE
10.1029/2018JF004655

Key Points:
- We examine and discuss implications of the unfrozen liquid water content on the long-term thawing of permafrost
- We demonstrate that the presence of material with substantial unfrozen liquid water content at below 0°(temperature can slow down thawing
- Futureobservation networks should try to incorporate measurements of the unfrozen liquid water content in the near-surface permafrost

Supporting Information:
- Supporting Information 51
- Table 51
- Table 52
- Table 53

Correspondence to:
D.J. Nicolsky,
djnicolsky@alaska.edu

Citation:
Nicolsky, D. J., & Romanovsky, V. E. (2018). Modeling long-term permafrost degradation. *Journal of Geophysical Research: Earth Surface, 123,* 1756-1771. https://doi.org/10.1029/2018JF004655

Received 21 FEB 2018
Accepted 13 JUN 2018
Accepted article online 22 JUN 2018
Published online 14 AUG 2018

Modeling Long-Term Permafrost Degradation

D.J. Nicolsky[1] and V.E. Romanovsky[1,2,3]

[1]Geophysical Institute, University of Alaska Fairbanks, Fairbanks, AK, USA, [2]Earth Cryosphere Institute, Tyumen Scientific Centre SB RAS, Tyumen, Russia, [3]Department of Cryosophy, Tyumen State University, Tyumen, Russia

Abstract Permafrost, as an important part of the Cryosphere, has been strongly affected by climate warming, and a wide spread of permafrost responses to the warming is currently observed. In particular, at some locations rather slow rates of permafrost degradations are noticed. We related this behavior to the presence of unfrozen water in frozen fine-grained earth material. In this paper, we examine not-very-commonly-discussed heat flux from the ground surface into the permafrost and consequently discuss implications of the presence of unfrozen liquid water on long-term thawing of permafrost. We conducted a series of numerical experiments and demonstrated that the presence of fine-grained material with substantial unfrozen liquid water content at below 0°C temperature can significantly slow down the thawing rate and hence can increase resilience of permafrost to the warming events. This effect is highly nonlinear, and a difference between the rates of thawing in fine- and coarse-grained materials is more drastic for lower values of heat flux incoming into permafrost. For high heat flux, the difference between these rates almost disappears. As near-surface permafrost temperature increases towards 0°C and the changes in the ground temperature become less evident, the future observation networks should try to incorporate measurements of unfrozen liquid water content in the near-surface permafrost and heat flux into permafrost in addition to the existing temperature observations.

1. Introduction

Climate warming of the last half of a century resulted in many changes in all components of the Earth's system (Intergovernmental Panel on Climate Change [IPCC], 2013), including the Cryosphere. Permafrost, as an important part of the Cryosphere, has been also strongly affected (Romanovsky et al., 2010; Romanovsky, Yoshikawa, et al., 2010; Vaughan et al., 2013) by climate warming. Degradation of near-surface permafrost at some locations was observed as a result of climate warming (James et al., 2013; Romanovsky et al., 2013). However, large ice wedges near the ground surface are commonly found at sites with undisturbed surface conditions during construction projects in the interior of Alaska where the mean ground temperature of permafrost is higher than -1°C, despite several decades of the climate warming. These ice wedges are of the Late Pleistocene age and they survived the Holocene Thermal Maximum, which occurred in Alaska between 8,000 and 12,000 years ago when the air temperature was 1 or 2°c higher than now (Kaufman et al., 2004; Renssen et al., 2009). At other locations, where natural or human surface disturbances occur, permafrost first degrades relatively fast, but then its rate of thawing seems to decrease and becomes quite small (Calmels et al., 2012; Yoshikawa et al., 2002). Recently, Froese et al. (2008) and Reyes et al. (2010) implied a resilience of permafrost to degradation by reporting relict Middle Pleistocene ice wedges that were buried by volcanic tephra and consequently survived previous interglacial warming periods.

Romanovsky and Osterkamp (2000) related the lower rates of changes in relatively warm permafrost to the unfrozen water presence in frozen fine-grained earth material. However, we believe that an in-depth explanation of this phenomenon is warranted especially now when the changes in permafrost and specifically the rate of permafrost thawing were designated by IPCC (2013) as one of the major uncertainties in future climate projections.

The major driving force of permafrost warming and/or thawing is a long-term imbalance in incoming and outgoing heat fluxes at the upper boundary of permafrost integrated over a certain time period (Williams, 1982). If more heat is coming in than going out, permafrost will be warming and eventually thawing. If the opposite is true, permafrost will be cooling, the active layer could be converting into permafrost from the permafrost table up, and the thickness of permafrost may be increasing at the lower boundary of permafrost, although at a very slow rate. This heat imbalance at the permafrost table as well as the partial thawing of the interstitial ice inside the permafrost is difficult to measure directly. Therefore, to investigate and explain the above-mentioned phenomena and to examine heat flux from the ground surface into the permafrost, we present several numerical modeling case studies. We demonstrate that the presence of fine-grained material with substantial unfrozen liquid water content at below 0°C temperature can significantly slow down the thawing rate, and hence can increase resilience of permafrost to the warming events. Results of our efforts show that, depending on a specific shape of the unfrozen water content curve in soil, permafrost thawing and a talik formation triggered by atmospheric warming may be delayed in fine-grained soils if compared to mineral soils of coarse-grain texture, such as sands or gravels. We believe that any representation of permafrost in global or regional climate models should include the thermal effects of unfrozen water in soils. Otherwise, the rates of permafrost thawing and degradation produced by these models will not be realistic.

Physical effects due to the presence of unfrozen liquid water in the freezing ground are mentioned by Williams (1967) and Anderson and Morgenstern (1973) and are now incorporated into many numerical models (Best et al., 2011; Cox et al., 1999; Oleson et al., 2008); however, an influence of unfrozen liquid water content on the overall permafrost dynamics is rarely fully examined. For example, Romanovsky and Osterkamp (2000) mention that the unfrozen liquid water content retards freezing of the active layer and that these effects can last from a few weeks to several months. However, much less attention so far, and in Romanovsky and Osterkamp (2000), in particular, was given to the process of long-term thawing of permafrost in fine-grained material. In this paper, we thoroughly examine permafrost dynamics under various ground surface conditions, for example, a small and large heat flux at the ground surface, and discuss implications of the unfrozen liquid water content on the long-term thawing of permafrost. Furthermore, we investigate a nonlinear dependence of the permafrost thawing on an amplitude of the incoming heat flux and provide estimates of the heat flux into the permafrost based on observations in Alaska.

The structure of this paper is as follows. In section 2, we scrutinize temperature observations collected at three sites in the interior of Alaska and estimate a long-term heat flux into permafrost due to natural climate warming. Section 3 introduces the numerical model of permafrost dynamics and describes results of the conducted sensitivity study. Two scenarios of the permafrost degradation are studied. In both scenarios, the ground material was considered to be homogeneous and a constant heat flux was applied at the ground surface. In the first case, the permafrost degradation is modeled under the natural climate conditions, while in the second case the permafrost degradation due to the disturbed ground surface conditions is examined. To supplement the above scenarios, we also considered a two-layer soil column and different boundary conditions. Similarities and differences between cases were revealed. Finally, in section 4, we discuss the implications of the fact that unfrozen water content dynamics may effect permafrost degradation under climate warming and state conclusions.

2. Ground Temperature Observations

While studying the subsea permafrost, Nixon (1986) noted that the thawing rate for saline frozen ground material decreases in numerical experiments, in which the phase change is not confined to a discrete freezing temperature. Later, Romanovsky and Osterkamp (2000) also conjectured that freezing of the active layer and thawing of permafrost slows down due to phase change processes occurring in a range of temperatures. In this section we thoroughly examine the University Farm site (Figure 1), which was briefly discussed in Romanovsky and Osterkamp (2000), and analyze physical mechanisms responsible for the observed temperature dynamics.

The University Farm site (-147°51'27.1"W, 64°51'10.4"N) is located on a higher bench of the Chena River floodplain, in the discontinuous permafrost region with a mean annual ground temperature about -1°C. In the 1930s an area around the site was cleared of vegetation to support agricultural activities, which have been taking place each year since then. As a result of disturbances to the natural surface conditions, the permafrost started to thaw and a 10-m-thick talik above permafrost appeared by the early 2000s (Romanovsky & Osterkamp, 2000). Currently, the talik penetrates to the depth of 12.5 m and the thickness of the seasonally frozen layer is typically between 1.2 and 1.8 m. The daily temperature in the seasonally frozen layer and shallow parts of the above-permafrost talik are monitored at 14 different depths down to 3 m, while the ground temperature up to the depth of 20-40 m are measured once a year with a precision of 1/100°C.

The borehole temperature measurements at the University Farm site from 1986 to 2012 are depicted in Figure 2a. All temperature observation data used in the analysis are provided in the supporting information. One may notice that the shape of the temperature profile remains approximately the same. We recall that

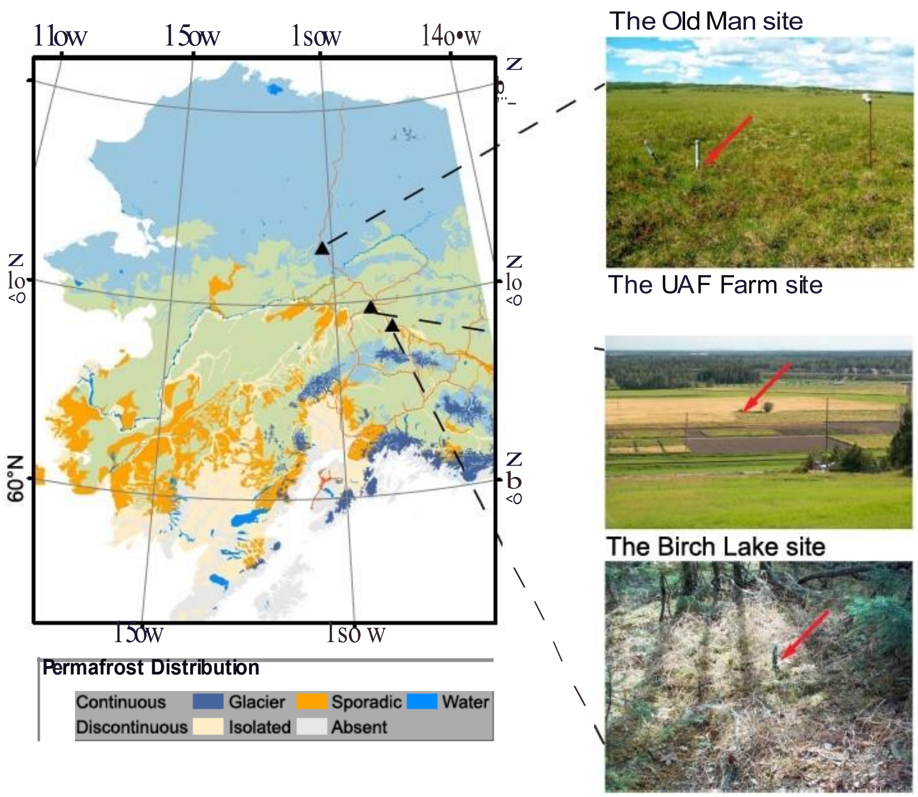

Figure 1.Left: A map of the permafrost characteristics in Alaska (Jorgenson et al., 2008).Locations of the ground temperature monitoring sites are shown by black triangles on the map. Right Location of the borehole is shown by the red arrow.Additional information and photographs could be found at http://permafrost.gi.alaska.edu.

Romanovsky and Osterkamp (2000) pointed out that a persistent curvature of the temperatu re profiles in the upper part of permafrost isdue to the presence of unfrozen liquid water, which introduces distributed latent heat sink over the curved portion of the temperatu re profile. To estimate the unfrozen liqu id water content (} = 8(T) distribution with depth for each year, we employ a parameterizat ion by Tice et al. (1989), that is, 8(T) = (pb f Pw) W(T).Here W(T) = al Tlb isthe unfrozen water content weight in percentage of dry sample, Pb is the dry sample density, and Pw = 1,000 kg/m^3 is the density of water. The constants Pb = 1,170 kg/m^3, a = 0.064, and b = -0.43 are related to the undistu rbed Fa irbanks silt (Tice et al., 1989); the maximum unfrozen liqu id water content (} is limited by the soil porosity 1/ = 0.4 m^3/m^3.Substituting the measured temperature profiles into the above formula,we obtain the unfrozen liqu id water content (} profiles for each year. The estimated unfrozen water profiles are illustrated in Figure 2b. One could notice that the h ighest curvature in the temperatu re profilers occurs when (} is between 0.15 and 0.2 and likely corresponds to an active dissipation of the heat flux in the upper part of permafrost. To support this hypothesis we compute the heat flux from the warmer talik towards the colder permafrost for each temperatu re profile. The heat flux isestimated by computing the temperature gradient with respect to depth and multiplying it by the value of thermal conductivity A. dependent on the value of 8, according to Romanovsky and Osterkamp (2000).To avoid clutter we do not plot heat flux in the talik and only show the heat flux distribution in permafrost in Figure 2c. Note the heat penetrates from the talik into permafrost and is at least 0.15-02 W/m^2; however, the latter significantly depends on the year when the permafrost temperature measurements were taken. We stress that the depicted plots represent instantaneous profiles of the heat flux; we estimate long-term mean annual values later in the manuscript.

We hypothesize that the presence of the fine-grained material in the soil man ifests itself in the elevated unfrozen water content in the soil and hence allows a significant portion of the heat flux to penetrate through the permafrost boundary into its body. The penetrated heat is then expended both to raise the temperature and to partially melt some of the interstitial ice at the sub O•C temperature range inside of the permafrost body. However, it is rather difficult to verify this hypothesis in natural experiments, because finding two sites with the same surface energy balance and physica l properties of the ground material, but different unfrozen

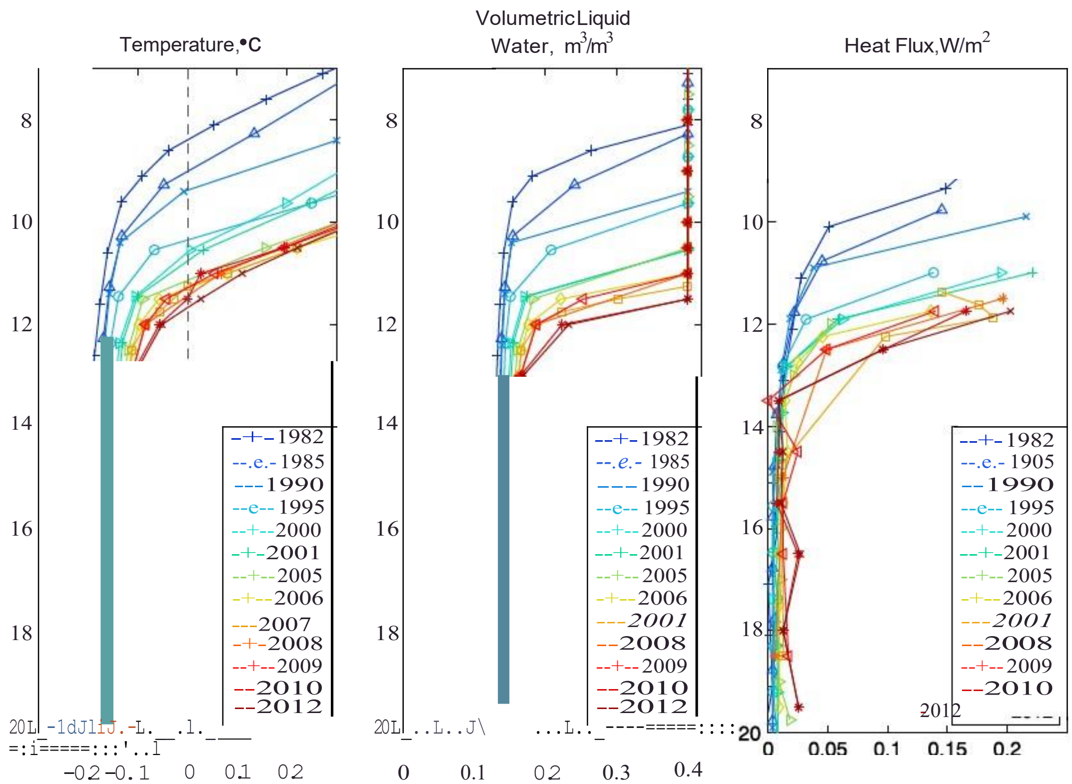

Figure 2. Measured temperature profiles at the University Farm site (a), the estimated unfrozen liquid water content corresponding to temperature profiles (b), and the estimated annual heat flux (C).

water content characteristics is almost impossible. Therefore, in the next section we consider two hypothetical numerical experiments that can help us to support our hypothesis. Before proceeding further, we note that the University Farm site does not represent typical conditions, due to the anthropogenic surface disturbances. Therefore, in order to determine plausible long-term heat flux entering from the ground surface into the body of permafrost from the ground surface, we consider two sites with the natural surface conditions, where long-term observations of permafrost have been conducted (Osterkamp, 2003).

In this study we use data from two sites along the North-South transect of Alaska, namely, the Old Man (-150°37'7.7"W, 66°27'0.7"N, a wide subarctic valley floor covered by a wet tussock tundra) and Birch Lake (-146°41'17. 'W, 64°19'24.7"N, a black spruce forested area with permafrost) sites (Figure 1). Both of these locations are good representatives of permafrost conditions in the Interior Alaska. The thermal state of permafrost at Old Man and Birch Lake has been monitored along the 60-m-deep boreholes once a year since the 1980s (Osterkamp, 2003). In Figure 3, for each site, we depict three temperature profiles measured approximately at the same time of the year, but with an approximately 10-year difference between the measurements. We note that the temperatures at the Old Man site exhibit a steady warming, while the permafrost at Birch Lake showed a bit more complicated behavior: rapid warming followed by a cooling and then a very recent warming again (Romanovsky et al., 2015). Nevertheless, the Birch Lake site illustrates a long-term warming trend from the 1980s to the 201 Os. Changes between the selected temperature profiles allow us to estimate the mean annual heat flux $\mathcal{F}$ penetrating into the permafrost from the ground surface. Note that the heat is being spent to increase the ground temperature $T=T(z,t)$ and also to melt interstitial ice and hence the mean heat flux $\mathcal{F}_{t_1\to t_2}$ between moments t_1 and t_2 at z_t = 2 m depth could be approximated by

$$\mathcal{F}_{t_1\to t_2} = \frac{1}{t_2-t_1}\int_{z_t}^{z_b} \left[\left(L\theta(z,t_2)+C(z,t_2)T(z,t_2)\right) - \left(L\theta(z,t_1)+C(z,t_1)T(z,t_1)\right)\right]dz,$$

where L is the latent heat of fusion and $C = C_i + (C_w - C_i)\theta$ is the volumetric heat capacity of the ground material (Nicolsky et al., 2009). The quantity C_i is the volumetric heat capacity of completely frozen ground material, and subscripts w and i mark the properties of water and ice, respectively. The value of z_b equals a depth, where the temperature change over the time interval $[t_1, t_2]$ is negligibly small.

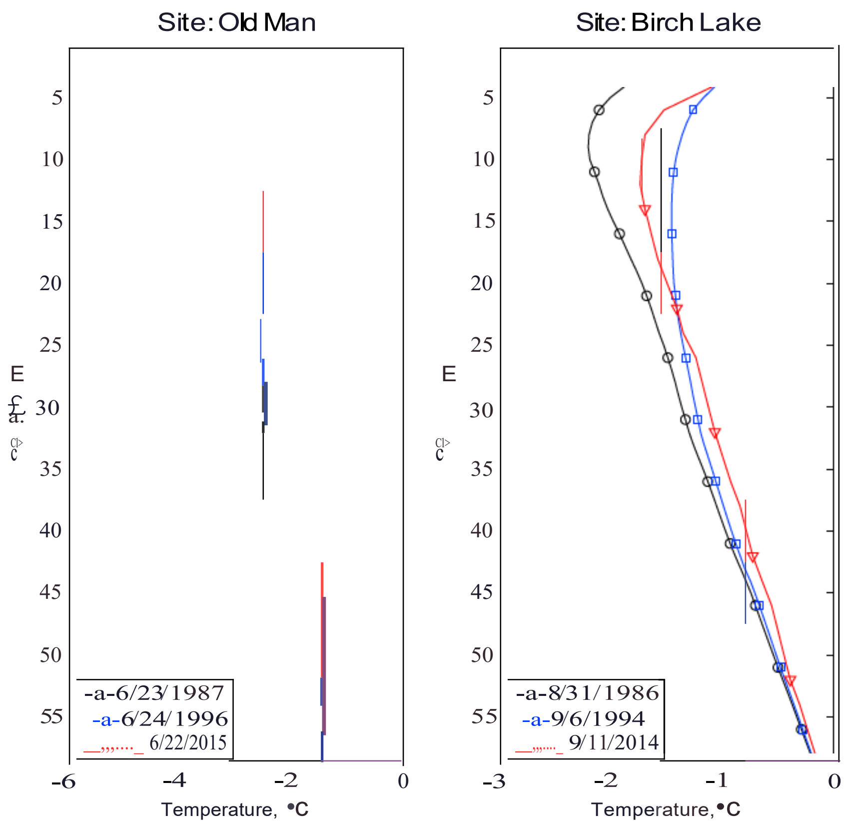

Figure 3. Measured temperature profiles at the Old Man (a) and Birch Lake (b) sites.

For the Birch Lake site, the temperature does not significantly change at z_b = 60 m during the period of measurements, while for the Old Man site, z_b >60. Since the temperature measurements are not available deeper than 60 m at the Old Man site, the value of *r* computed for z_b = 60 m provides a lower bound for the mean heat flux at the Old Man site. Besides limitations in finding *r* due to availability of the ground temperature observations, the largest uncertainty in computing *r* is associated with estimation of the unfrozen water *content (}* for the ground material experiencing the largest temperature warming between $t = t_1$ and *ti*. A contribution of the uncertainty in (} for the ground material, at a significant depth, where *T(z, ti) - T(z,* t_1) 0, is considered small because the uncertainty is multiplied by a rather negligible difference in temperature.

Recall that (} is the volumetric unfrozen liquid water content and its value depends on the temperature, soil texture, salinity, content of the organic material, and other factors (Anderson & Morgenstern, 1973; Lovell, 1957). In many physical circumstances, the value *of (}* could be parameterized with respect to temperature and soil porosity *T/* as *8 = 11</>,* where </>(T) = ITfr.1-b is the liquid pore water fraction (Anderson & Morgenstern, 1973; Hobbs, 1974); however, values of the freezing point depression r.< 0 and constant *b* > 0 are unknown for many sites in Alaska. Small values of *b* describe the liquid water content in fine-grained soils, whereas large values of b are related to coarse-grained materials in which almost all water freezes at the temperature r•.

For the silty soils, found near the ground surface at the Birch Lake and Old Man sites, we assume the value of *b* E [0.5, ..., 0.8] and r. E [-0.05, . . . , -0.01] that result in the spread *for </>* shown in Figure 4. The assumed spread in *(}* is comparable to that reported in Tice et al. (1989, Figure 2) for the Fairbanks silt. Unfortunately, a lower extent of the silt horizon at the Birch Lake and Old Man sites is unknown. The silt is likely underlined by coarse grained material, the unfrozen water content of which is parameterized by steep curves in Figure 4. Since most of the ground temperature warming at both sites occurred in silty soil in the upper 20-25 m, we assume that the uncertainty in (} related to gravel, if any exists at the sites, is rather small.

Besides the uncertainty in the unfrozen water content, there is an uncertainty in the parameters *T/* and C. According to previous investigations (Nicolsky et al., 2007, 2009; Romanovsky & Osterkamp, 2000) we assume that the range of variability for the soil porosity *T/* is [0.3 ...0.4] m^3/m^3, and the volumetric heat capacity *C,*

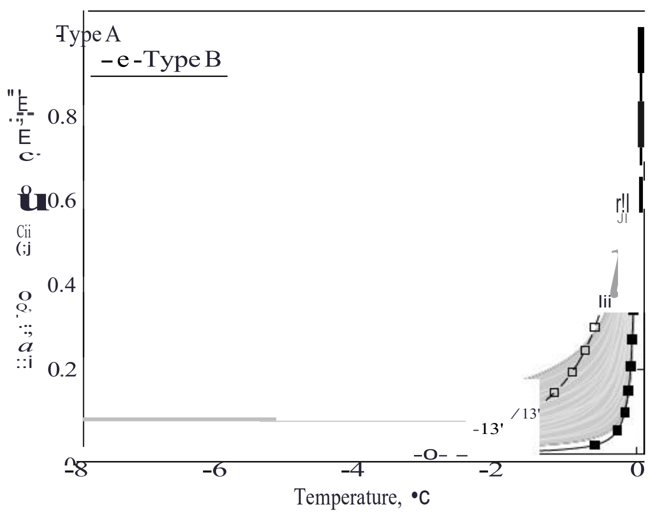

Figure 4. Gray shaded area illustrates an uncertainty in the liquid pore water fraction ϕ for the silt material at the Birch Lake and Old Man sites. Dashed and solid lines show parametrization of ϕ considered in the sensitivity study.

for the frozen material is constrained within $[1.4\text{-}1.7]\cdot 10^6$ [J/m^3/K]. Consequently, for the Old Man site we find that the mean value of the annual heat flux between 1987 and 1996 is $\mu_{1987\to1996} = 0.13 \pm 0.07$ W/m^2, and the values of the heat flux between 1987 and 2015 is $\mu_{1987\to2015} = 0.15 \pm 0.08$ W/m^2. This implies that the permafrost is steadily getting warmer and its temperature is increasing. At the other location, that is, at the Birch Lake site, the mean annual heat flux between 1986 and 1994 is $\mu_{1986\to1994} = 0.39 \pm 0.24$ W/m^2, while the mean value between 1986 and 2014 is $\mu_{1986\to2014} = 0.15 \pm 0.09$ W/m^2. This leads us to conclude that the period from late 1980s to mid-1990s is characterized by a substantially larger heat flux, if compared to the one from late 1980s to mid-2010s. Both sites, that is, Birch Lake and Old Man show a long-term warming of the ground material with a mean annual heat flux penetrating into the permafrost from the ground surface in the range of 0.2 ± 0.1 W/m^2.

Some rough estimates of the heat flux into the surface of the permafrost from 1990s to early 2000s were obtained by Osterkamp et al. (2009) for a site near Healy, Alaska, using thaw settlement and estimations of the ground ice content. Osterkamp et al. (2009) estimated that during that period the net annual heat flux was at least 0.4 W/m^2; however, after the 2000s permafrost degradation at the Healy site decelerated until recently and we conjecture that 0.4 W/m^2 was a local response similar to that observed at the Birch Lake site. Evidence for a cyclic variation of permafrost temperatures in northern Alaska is also presented by Osterkamp et al. (1994). Therefore, in the following numerical experiments we assume that the long-term heat flux into permafrost could be assumed to be equal to 0.2 W/m^2.

3. Modeling Methods and Sensitivity Study

The permafrost temperature dynamics are commonly simulated by a 1-D heat equation with phase change (Carslaw & Jaeger, 1959):

$$C\frac{\partial T}{\partial t} + L\frac{\partial \theta}{\partial t} = \frac{\partial}{\partial z}\left(\lambda \frac{\partial T}{\partial z}\right). \qquad (1)$$

where $\lambda = \lambda_*(\lambda_w/\lambda_i)^{\theta}$ stands for the thermal conductivity of the ground material (Nicolsky et al., 2009). Similar to the definition of the volumetric heat capacity C_*, the quantity λ_* stands for the thermal conductivity of the completely frozen material and the subscripts w and i mark the properties of water and ice. We refer the reader to Nicolsky et al. (2009) for further details and numerical solution to the above heat equation. An accuracy of the numerical scheme, which was used to model thawing of the ground material with unfrozen liquid water content is tested in Appendix A.

To illustrate effects of the long-term heat flux into the permafrost, we simulate temperature dynamics in a 150-m-thick soil column, that is, $z \in [0, 150]$, and at the top of the soil column $z = 0$ impose the Neumann boundary condition $\lambda \nabla T(0,t) = \mu$, where μ is the long-term heat flux into the ground material. To highlight

Table 1
Numerical Experiments Witha Homogeneous Soil Column and a Constant Heat Flux μ at the Ground Surface

	Unfrozen liquid water content parameter ization	Heat flux μ,[W/m^2]
Coarse-gra ined sediments, natural surface conditions	Type A	$\mu = 0.2$
Fine-grained sediments natural surface conditions	Type B	$\mu = 0.2$
Coarse-grained sediments, disturbed surface conditions	Type A	$\mu = 1$
Fine-grained sediments, disturbed surface conditions	Type B	$\mu = 1$

the effects of redistribut ion of heating from the surface into the ma in body of permafrost,we assume that the geothermal heat flux at the bottom of the soil column z = 1SO iszero.

In the following numerica l experiments, we employ two idealized unfrozen liquid water content curves *8,* plotted by dashed and solid lines in Figure 4. Both of the displayed parameterizat ions have a freezing point depression at T very close to O•C,meaning that ice does not exist in the soil pores if $T>0$.The Type A parameterization describes the liquid water content in coarse-gra ined material, in which most of the liquid water freezes atthe temperatu re T,whereasthe Type B pa rameterization isrelated to fine-grained soils, where some significant unfrozen liquid water content exists at -1•C. Note that for both parameterizat ions, we assume that the unfrozen liqu id water content vanishes when temperature approaches -S°C. The latter assumption is only imposed for the clarity of the presentation and could be omitted while considering other cases.

To distill the essence of how unfrozen liquid water content affects the thawing of permafrost, we consider homogeneous soil columns. Although examining heterogeneous soil columns with varying soil temperatures could be more rea listic (as considered later in the manuscript), but interference from effects arising from the nonuniform initial conditions and soil properties parameter izations could make the underlying analysis difficult. To this effect, if possible, we try to examine homogeneous soil columns and the ground material is assumed to be initially at a constant temperature T_0 = -S°C, that is, all water in the soil pores is frozen and it will require an equal amount of energy for the soil columns to reach the same constant temperature above 0°C.

A summary of the numerical experiments with a constant heat flux specified at the ground surface is provided in Table 1. In each experiment, we prescribe properties of the ground material according to those listed in Table 2 and then simulate the temperature dynamics for 500 years. In the first two experiments, we assume that the long-term heat flux is $\mu = 0.2$ W/m^2 that corresponds tothe above-mentioned sites, while in the other two experiments, we simulate a rather high long-term heat flux $\mu = 1.0$ W/m^2 that corresponds to severe natu ral surface disturbances or a very substantial climate warm ing. Note that the amount of latent

Table 2
Soil Properties af the Ground Material

Property	Value
Porosity, *11*	0.35 (m^3/m^3)
Thermal conductivity of the completely frozen material, *A[*	2.3 (W/m/K)
Thermal conductivity of the thawed material, *At*	1.4 (W/m/K)
Thermal conductivity of ice, *A/*	2.2 (W/m/K)
Thermal conductivity of water, *Aw*	0.56 (W/m/K)
Volumetr ic heat capacity of the completely frozen material, *Ct*	1.s . 1O^6(J/m^3/K)
Volumetr ic heat capacity of the thawed material, C_1	2.3 · 10^6(J/m^3/K)
Volumetr ic heat capacity of ice, C_1	1.9 · 10^6(J/m^3/K)
Volumetr ic heat capacity of water, *Cw*	4.2 · 10^6(J/m^3/K)

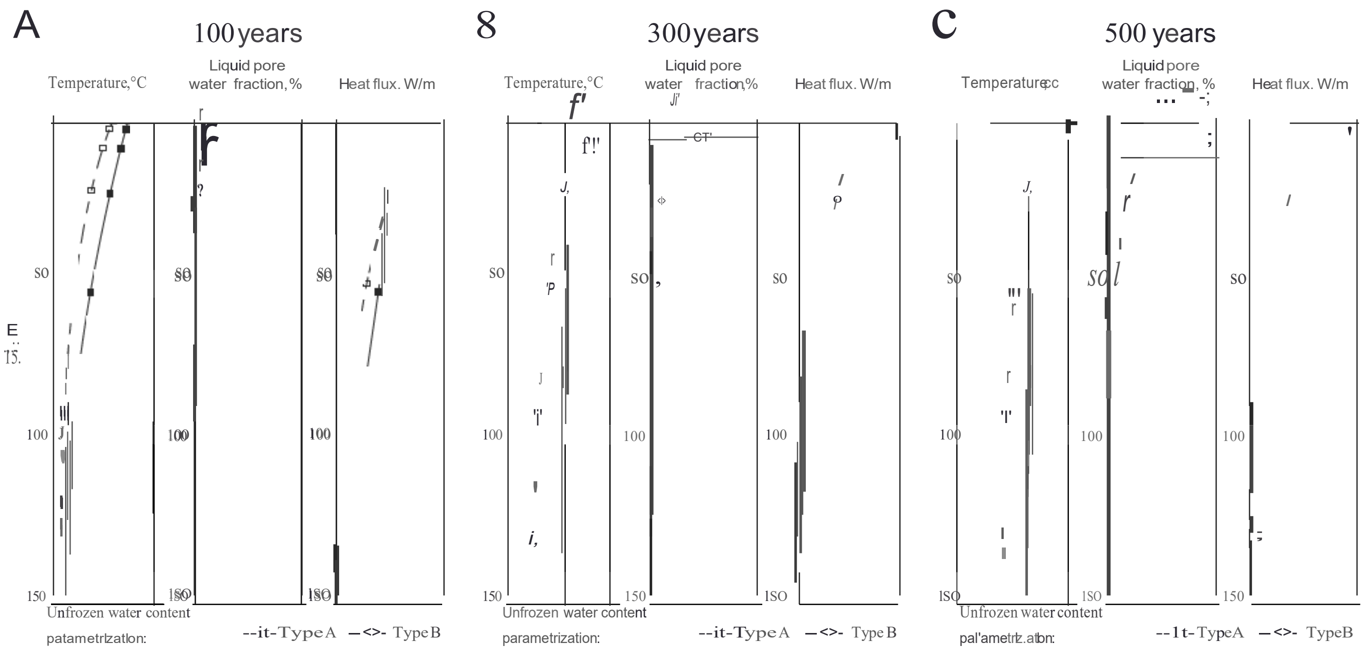

Figure S.Modeled temperature; unfrozen liquid water content; and heat flux after 100, 300, and 500 years after the long-term heat flux $\mu = 0.2$ W/m^2 is applied at the surface of the soil column. Numerical results related to the Type A and B parametrizations are plotted by solid and dashed lines, respectively.

and sensible heat initially stored in the soil column in each subcase is exactly the same, since the soil at $T_0 = -5°C$ is completely frozen, that is, $\theta = 0$. Next, we analyze how the long-term heat flux into the soil column is heating the ground material and thawing the interstitial pore ice with time.

3.1. Homogeneous Soil Column, Natural Surface Conditions: $\mu = 0.2$ W/m^2

In this subsection, we present numerical results related to the long-term heat flux $\mu = 0.2$ W/m^2 corresponding to natural conditions. Figure S shows the simulated profiles of the temperature T, unfrozen water content θ, and the heat flux $A.'*$ after 100, 300, and SOO years of the simulation. The modeling results related to Types A and B parametrizations of the unfrozen liquid water content are plotted by solid and dashed lines, respectively.

After 100 years, we note that for the Type A parametrization (most of the water freezes at a near-zero temperature), the simulated permafrost temperature at the surface almost reaches the freezing point depression T_* and the liquid pore water fraction ϕ, shown by the solid line, reaches 70% near the surface; note that the value of ϕ remains very close to zero for the rest of the soil column. At the same time, in the simulation related to the Type B parametrization (the phase change occurs over a wide range of temperatures) the near-surface unfrozen water content, shown by the dashed line, is lower at the ground surface, but is higher than that for the Type A content for $z > 5$ m. We also note that the temperature across the entire soil column for the Type B parameterization is lower if compared to the temperature computed for the Type A parameterization (see Figure Sa).

We conclude that the long-term heat flux, in the numerical experiment with the Type B parameterization, is used to melt some interstitial ice and somewhat to raise the ground temperature. Whereas in case of the Type A parametrization, the heat flux is primarily used to raise the soil temperature -Note that at 7S m depth, for results with the Type A parametrization, the modeled ground temperature is 1°C warmer and the heat flux is higher by 0.2S W/m^2. We thus conclude that at the initial stage of thawing in the numerical experiment with the Type A parametrization, the heat flux penetrated deep into the permafrost and most of it is absorbed by raising the ground temperature to a freezing point depression T_*, while the interstitial ice is mainly preserved. After a certain time, only when the ground temperature approaches 0°C, the heat flux is used for the phase change processes near the thawing front in the numerical experiment with the Type A parameterization.

After 300 years, in the numerical experiment with the Type A parametrization, near-surface ground temperature is close to 0°C and a 10-m-thick talik appears, in the rest of the soil column the ground temperature is higher than -2C°C (see Figure Sb). In the numerical experiment with the Type B parameterization, the ground surface temperature just arrived at 0°C, and a talik is not yet developed. Dynamics of the talik

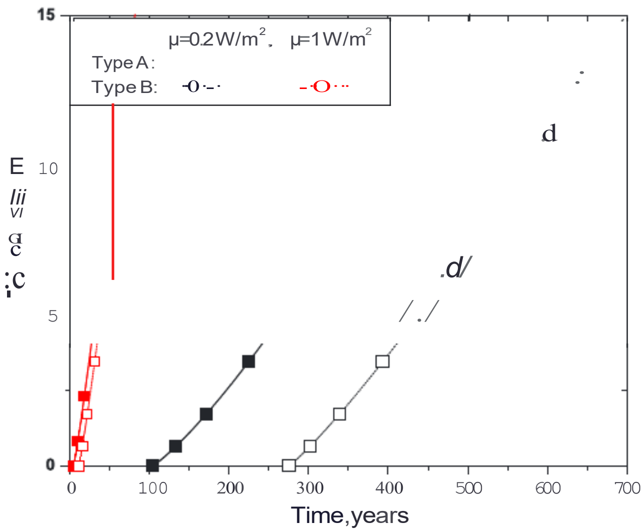

Figure 6. Modeled talik thickness in case when the long-term heat flux μ is applied at the surface of the soil column. Numerical results related to the Types A and B parametrizations are plotted by solid and dashed lines, respectively.

thickness for both experiments are shown in Figure 6 by black lines. We emphasize that in the experiment with the Type B parameterization, despite a significant delay in the development of a talik, the near-surface permafrost is already partially degradated and a considerable amount of the interstitial ice has melted. The reader is also encouraged to compare the liquid pore water fraction profiles in Figure S. Analysis of the heat flux profiles also reveals another significant difference between the experiments. The heat flux plots for the Type A parametrization strengthens our hypothesis that most of the long-term surface heating is primarily absorbed at the upper boundary of thawing permafrost and is responsible for melting the interstitial ice just beneath the talik. Only about 2S% of the long-term heat flux penetrates below the 2S m depth and expends as a sensible heat for further warming of deeper permafrost. For the Type B parametrization, the modeled heat flux is a less rapidly decreasing function with depth and practically all surface heating penetrates into the permafrost and expends as both sensible and latent heat for further warming of permafrost and for melting interstitial ice respectively.

After SOO years, a talik is developed in both numerical experiments (see Figures Sc and 6). However, the thickness of the talik in the experiment with the Type A parametrization is almost twice larger, as could be noticed in Figure 6. As in the previous snapshot, the curvature of the liquid pore water fraction profile is similar to the curvature of heat flux profile and these curvatures are smaller in the experiment with Type B parameterization. Therefore, as 200 years earlier, the incoming long-term heat in the experiment with the Type A parametrization is primarily spent on the water phase change transition in a thin region just below the top of thawing permafrost. The ratio of heat fluxes corresponding to these two numerical experiments is about two times at 2S-SO m. A larger amount of heat penetrates deep into the permafrost in the experiment with the Type B parametrization and causes a larger percentage of the interstitial ice to melt, as shows on the corresponding liquid pore water fraction profile (see Figure Sc).

3.2. Homogeneous Soil Column, Disturbed Surface Conditions: $\mu = 1\,W/m^2$

In this section, we present numerical results in the case when the long-term heat imbalance is rather large, that is, $\mu = 1\,W/m^2$. Recall that this value of heat flux corresponds to sites with severe natural surface disturbances or when a very substantial climate warming occurs. Similar to the previous set of experiments, shown in Figure S, we plot temperature, liquid pore water fraction, and heat flux profiles exactly at the same moments of time. We emphasize that the case of $\mu = 1\,W/m^2$ is considered to highlight a nonlinear response of ground temperature to changes in the incoming energy.

Numerical experiments indicate a development of the talik after 100 years of heating, as shown in Figure 7a, much quicker than in the previous set of experiments. Dynamics of the talik thickness for both experiments are shown in Figure 6 by red lines. Now in both experiments, the computed temperatures and liquid pore water fractions decrease very sharply at the upper surface of thawing permafrost approximately at a 20-m depth. Despite these similarities, in the numerical experiment with the Type B parametrization, the modeled talik is still about 10% shallower. The latter can be explained due to some slightly different profiles of the heat flux. Note that the curvature of the heat flux profile for the Type B parameterization just below the upper permafrost boundary is still smaller than that for the Type A parameterization. From the physical point view, it means that the heat still penetrates deeper and causes more interstitial ice thawing in the experiment with the Type B parametrization. However, this difference in curvatures is not as pronounced as in the above-considered case for $\mu = 0.2\,W/m^2$.

The simulated temperature, water fraction, and heat flux profiles after 300 and SOO years of ground heating, as shown in Figures 7b and 7c, respectively, display that the taliks in both numerical experiments are getting much thicker than in the case of $\mu = 0.2\,W/m^2$. Most of the incoming heat flux is being utilized to melt ice at the upper boundary of thawing permafrost. Nevertheless, the talik modeled with the Type B parametrization still remain shallower by approximately S-7% because some heat still propagates down into the main body of permafrost. The reader may inspect heat flux profiles and note that their curvatures are higher for the Type A parametrization.

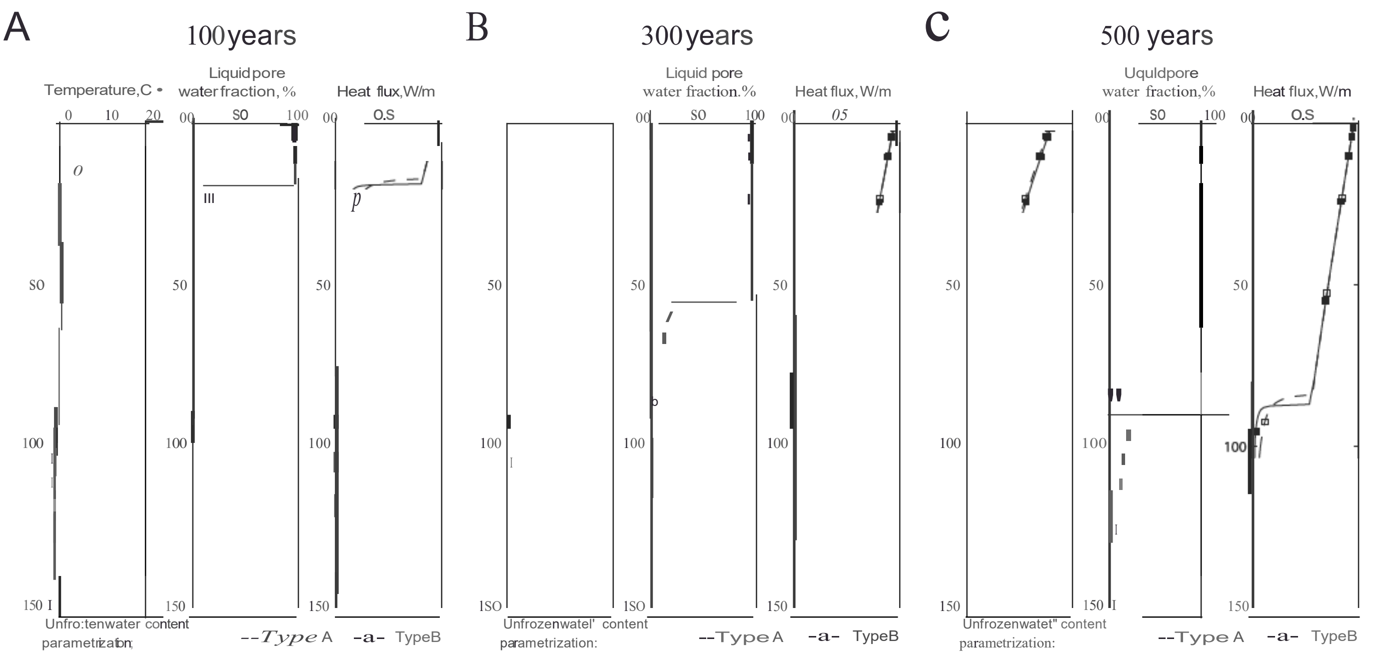

Figure 7.Modeled temperature; unfrozen liquid water content; and heat flux after 100, 300, and 500 years after the long-term heat flux μ = 1 W/m^2 is applied at the surface of the soil column. Numerical results related to the Types A and B parametrizations are plotted by solid and dashed lines, respectively.

The provided results indicate that the difference between two types of unfrozen water parameterization in locations of the upper boundary of thawing permafrost for large values of the ground surface heating is not as much pronounced as for the small values of ground surface heating; however, the differences might accumulate over time. In the next section, we will discuss physical implications of the fine-grained material and melting of the interstitial ice on thawing of permafrost and its recovery after a disturbance.

3.3. Two Layer Soil Column, Constant Ground Surface Temperature: T_s = O.S°C

In the above set of experiments, listed in Table 1, we investigated how properties of the subsurface material can modify the rate of permafrost temperature increase and the rate of permafrost thawing due to some idealistic warming scenarios. Specifically, how the unfrozen water content at below O°C and thermal conductivity of soil can modify the rate of permafrost warming and thawing. One of the limitations of the above numerical experiments is that a homogeneous soil column is examined and a constant heat flux is imposed on its top surface. To supplement the above investigations, we consider four additional numerical experiments, listed in Table 3. In these additional experiments, instead of prescribing the incoming heat flux, we now specify the constant temperature Ts = O.S°C at the ground surface. The initial ground temperature is likewise assumed to be -S°C.

In the first two experiments we consider a homogeneous mineral soil column, while in the other two, we consider a two-layer soil column with a 0.5-m-thick insulative layer with At = 0.8(W/m/K) on top of the mineral soil. Values of the thermal properties for the mineral soil are listed in Table 2. For the sake of simplicity, the heat capacity **C**, and porosity $T/$ of the insulative layer are assumed to be equal to those of the mineral soil. We also note that Experiments 1 and 3 are conducted, assuming that the soil column is composed of the coarse-grained ground material with the Type A parameterization, while Experiments 2 and 4 areorchestrated

Table 3
Numerical Experiments With the Constant Ground Surface Temperature Ts = OS°C *at the Ground Surface*

	Unfrozen liquid water parameterization	Soil column composition
Experiment 1	Type A	Mineral soil
Experiment 2	Type B	Mineral soil
Experiment 3	Type A	Insulative layer above the mineral soil
Experiment 4	Type B	Insulative layer above the mineral soil

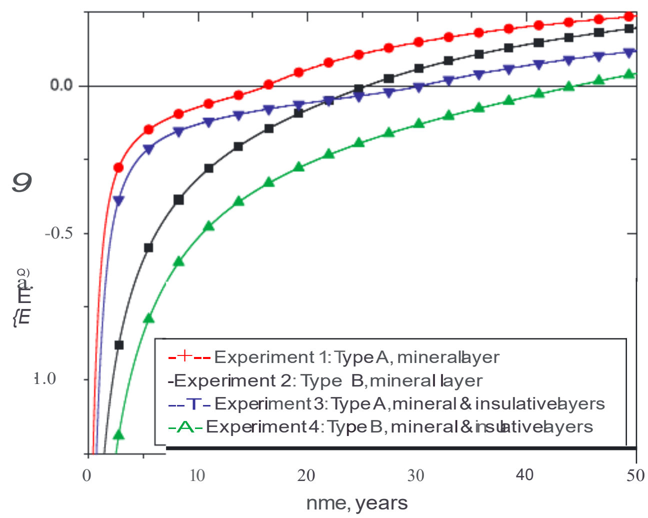

Figure 8. Comparison of the modeled ground temperature dynamics at the 2 m depth for numerical experiments with and without the 0.5-m thick insulative layer. Physical properties of the mineral layer are listed in Table 2; thermal conductivity λ_f for the insulative layer is 0.8 W/m/K). The heat capacity C, and porosity η of the insulative layer are assumed to be equal to those of the mineral soil.

assuming the fine-grained material-the Type B parameterization for the unfrozen liquid water content. After modeling permafrost degradation, we plot temperature dynamics at the 2 m depth in Figure 8. The figure caption summarizes differences between the four conducted experiments. One may note that in Experiment 1, the ground temperature at the 2 m depth quickly raises and reaches 0°C after 16-17 years, whereas in Experiment 2, the temperature increases more slowly and reaches 0°C only after 25-26 years. Due to the presence of the insulative material, in Experiments 3 and 4, the ground temperature raises and reaches 0°C at the 2 m depth even more slowly, that is, after 30-31 and 44-45 years, respectively. It is interesting to note that the effect of the insulative layer in Experiment 3 is comparable to an effect of the temperature distributed phase change, as simulated in Experiment 2. This comparison alone highlights the importance of effects related to the unfrozen liquid water content in the numerical calculations.

4. Discussion

In this manuscript, we analyze the influence of unfrozen liquid water on permafrost thawing and redistribution of the incoming heat flux. We stress that the goal of this study was to demonstrate that the presence of the unfrozen liquid water in fine-grained sediments whose temperature is below 0°C promotes propagation of the larger portion of the heat flux from the permafrost surface deep into the permafrost body. Furthermore, this heat causes partial thawing of the ground material, while the temperature remains below 0°C.

We also would like to emphasize the dependence of the permafrost thawing rate on the amount of heat supplied to permafrost due to climate warming. In contrast to many environmental variables determining an incoming heat flux at the ground surface (e.g., Oleson et al., 2013; Westermann et al., 2016), only two factors primarily define the heat flux into permafrost. The first one is the temperature difference between the ground surface and top of the permafrost. Another factor is the thermal properties of the ground material in the active layer. As the mean annual ground surface temperature, T_{95}, increases above 0°C, the temperature increase in the active layer is also subjected to the so-called thermal offset, ΔT_k, (Goodrich, 1978; Kudriavtsev & Melamed, 1972; Romanovsky & Osterkamp, 1995) and permafrost may be still stable when $T_{95} > 0$°C (Burn & Smith, 1988; Osterkamp & Romanovsky, 1999). However, further increases in T_{95} will be only partially compensated by the "thermal offset" (i.e., $T_{95} - \Delta T_k > 0$) and thus eventually lead to thawing of permafrost. The temperature compensation, ΔT_k, is less in a highly conductive well-drained, coarse-textured material such as sand or gravel (λ = 2.5-3.0 [W/m/K]) if it is compared to the heat propagation in the well-saturated, low-density organic material (λ = 0.2-0.3 [W/m/K]; Burn & Smith, 1988). Moveover, since the heat flux depends on the thermal conductivity, the higher the conductivity the larger heat flux we should expect if all other properties are equal. As a result, under the same surface warming conditions (e.g., an increase in temperature), the long-term heat flux into permafrost may be 10 times larger for mineral surfaces compared to the surfaces covered by a highly isolative thick layer of decomposed organic material. This fact can explain a well-known phenomenon of "ecologically protected permafrost" (Jorgenson et al., 2010; Shur & Jorgenson, 2007) when permafrost may survive a substantial warming for a long period of time in silty soils covered by a thick organic mat. The combination of Type B unfrozen water content curves in fine-grained or organic soils and the reduced long-term heat flux into permafrost together with a large negative thermal offset observed in fine-grained and organic soils (Romanovsky & Osterkamp, 1995, 2000) substantially delay the warming and thawing of permafrost in these conditions as it was demonstrated in our modeling experiments described in this paper. Alternatively, the higher rate of permafrost warming and thawing should be expected at the sites with coarse-grained material located right below the ground surface.

The impact of severe forest and tundra fires on permafrost mostly occurs through removal of moss and soil organic layer (Yoshikawa et al., 2002). Therefore, a long-term heat flux into permafrost may substantially increase due to the exposure of mineral ground, which was previously covered by a highly insulating thick layer of organic material. In our numerical experiments it will relate to an increase in the heat flux into permafrost from 0.2 to 1.0 (W/m^2). This increased heat flux may and in most cases does trigger a rapid warming and thawing of permafrost even in fine-grained soil. However, after several years or a decade of thawing, the permafrost table will become deeper by several meters (typically 3 to 5 m) and if permafrost is not extremely ice rich and the thaw will not trigger a deep surface subsidence, the thermal gradient between the ground surface and the top of permafrost will decrease enough to bring the long-term heat flux into permafrost to the original value of 0.2 (W/m^2). At this moment, the further thawing of permafrost in fine-grained material will slow down and may even stop because most of the heat will again go through the permafrost table to be used to melt the interstitial ice within the permafrost below its upper boundary as it was described in our numerical experiment with Type B soil parametrization. If the occurred pause in permafrost degradation will be long enough to re-establish the original surface vegetation and soil organic layer (i.e., restoration of the insulative layer on the ground surface) and the climate conditions are still suitable (i.e., no significant increase in the air temperature), then new permafrost can start to form and the talik, which was established after the disturbance, will disappear.

It is important to notice that while the interstitial ice may be actively thawing in the perennially frozen fine-grained sediments within a range of subzero temperatures (most typically between −1 and 0°C), the larger inclusions of pure ice, such as ice lenses, ice layers, and ice wedges, will not be melting at these temperatures, because their melting point is still exactly at 0°C. This massive ice will be preserved in permafrost for the entire period of time when the ground temperature will still be continuously below 0°C. As it was demonstrated in the numerical experiments, for example, see Figure 6, the lag of time between the beginning of a major warming at the ground surface and the time when the ground temperature will cross the 0°C threshold in the upper few meters of a fine-grained frozen sediment may be as large as several centuries. All climate change history during the Holocene is represented by a series of warmer and colder periods with the duration of each less than a few centuries (Lavrushin & Alekseev, 2005, p. 28). In this case, it is possible that the length of the relatively warm periods during the Holocene optimum were not long enough to start the process of rapid degradation of the massive Late Pleistocene ice wedges (Yedoma permafrost) at all locations within the Alaskan Interior. As a result, the Late Pleistocene Permafrost with massive syngenetic ice wedges imbedded into fine-grained silt sediment survived the time of the Holocene Optimum in many places around the Alaskan Interior where the present-day permafrost temperatures are typically ranged between −1 and 0°C. A similar reasoning may be established to explain the survival of pre-Late Pleistocene syngenetic permafrost during the previous interglacial (Froese et al., 2008).

5. Conclusions

The rate of permafrost thaw considerably depends on the texture of frozen ground via the amount of unfrozen liquid water trapped in soil pores. The rate of the downward thawing of permafrost for fine-grained materials could be significantly less than that for coarse-grained materials, given that all other factors are the same and the permafrost degradation just started. Furthermore, the rate is dramatically affected by the amount of the incoming heat flux. This effect is highly nonlinear and a difference between the rates is more drastic for lower values of the incoming heat flux. For the high heat flux, the difference between the rates of thawing of fine- and coarse-grained frozen materials almost disappears.

With the long-term rate of warming of 0.2 ± 0.1 W/m^2 (as recently observed in central Alaska, see section 2) it will take several hundreds of years for the present cold (-5°C or lower) continuous permafrost in the fine-grained material, to show a significant thaw. Therefore, any representation of permafrost in global or regional climate models should include the thermal effects of unfrozen water in soils. Otherwise, the long-term rates of permafrost thawing and degradation produced by these models will not be realistic.

As ground temperatures are increasing and reaching a distributive phase change zone -1...0°C, the temperature observation will become less informative than measurements of the unfrozen liquid water content and heat flux imbalance in the upper permafrost. The future observation networks should try to incorporate measurements of the unfrozen liquid water content and heat flux in the near-surface permafrost in addition to the existing temperature sensors.

Appendix A: Model Verification Studies

To verify accuracy of our numerical solution, we test it against an analytical solution to the heat equation (1). Many numerical schemes are commonly tested against the so-called Neumann solution (Gupta, 2003), which is derived under the assumption that the phase change occurs at the specific temperature, T_*, or

$$\theta = \begin{cases} 1, & T \geq T_* \\ 0, & T < T_*. \end{cases}$$

Here we present an analytical solution assuming that the phase change occurs in the range of temperature, which relates to freezing of the ground material with presence of the unfrozen liquid water below 0°C. The presented solution generalizes the Neumann solution to the heat equation with the temperature-distributed phase change process.

A.1. Derivation of the Generalized Neumann Solution

Similar to the assumption in the derivation of the Neumann solution, we suppose that the soil is a homogeneous mixture of soil particles and water at the temperature T_0. At time $t = 0$, the soil surface $z = 0$ is brought to the constant temperature T_s, which is indefinitely kept constant.

It is convenient to define the enthalpy H as

$$H(T) = \int_0^T C(s)ds, \qquad C(T) = c_s(T) + L\eta\frac{d\theta}{dT},$$

where the quantity C is commonly called the apparent heat capacity. Changing variables, equation (1) is transformed to

$$\frac{\partial H}{\partial t} = \frac{\partial}{\partial z}\left(D(T)\frac{\partial H}{\partial z}\right), \quad z > 0, \quad t > 0, \tag{A1}$$

where $D = \lambda/C$ is the diffusivity. Note that the equation (A1) admits a well-known Boltzmann-type similarity solution of the form $H(z,t) = \mathcal{H}(x)$, where the similarity variable is $x = z/2\sqrt{t}$, and similarity variable $\mathcal{H}$ satisfies the nonlinear ordinary differential equation (Klute, 1952; Philip, 1955)

$$-2x\frac{d\mathcal{H}}{dx} = \frac{d}{dx}\left(D(\mathcal{H})\frac{d\mathcal{H}}{dx}\right), \quad x > 0, \tag{A2}$$

while the initial and boundary conditions are transformed to $\lim_{x\to+\infty}\mathcal{H}(x) = 0$, and $\mathcal{H}(0) = 1$, respectively.

For soil, in which no phase change occurs, equation (A2) admits the solution in terms of the error function (Jaeger & Sass, 1964)

$$\mathcal{H}(x) = A\,\mathrm{erfc}\,(x/\sqrt{D}) + B,$$

where A and B are certain constants. Otherwise, equation (A2) is represented as a system of two first-order differential equations

$$\frac{d\mathcal{H}}{dx} = \frac{y}{D(\mathcal{H})}, \qquad \frac{dy}{dx} = -2x\frac{y}{D(\mathcal{H})}$$

that can be numerically solved using the shooting method (Kress, 1998). The equations is integrated from $x = 0$ to ∞, with the initial conditions $\mathcal{H}(0) = 1$ and $y(0) = a$, where a is a constant. Note that when $x \to \infty$,

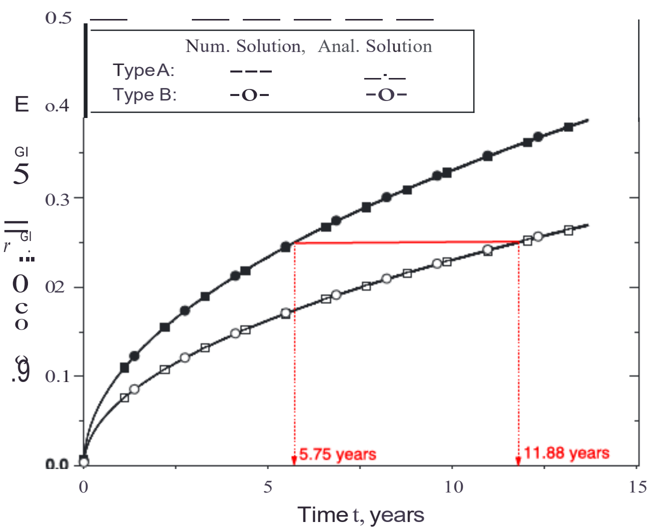

Figure A1. Comparison of the analytically and numerically computed location of the upper boundary of the permafrost.

H asymptotically approaches to a certain constant H_a, which value depends on a. Varying the constant a, it is possible to obtain that $H_a = 0$ and hence to solve the system of differential equations. To compute location of the T_* isotherm, we propose to use the following procedure. Given the value of T_* compute $H_* = H(T_*)$ and then find x_* such that $H(x_*) = H_*$. The location of the T_* isotherm is given by $2x_*\sqrt{t}$.

A2. Verification of the Numerical Scheme

To test the numerical scheme (Nicolsky et al., 2009) against the generalized Neumann solution, we consider a 50 m-thick soil column, discretized with spacing Δx 0.01 at the soil surface and exponentially increasing with depth. The soil thermal properties and the spatial discretization of soil column are exactly the same as those used in the sensitivity study (section 3).

As in the sensitivity study, we assume that the ground material is initially at -5°C temperature. But, instead of prescribing the heat flux at the ground surface $z = 0$, we set the temperature such that $T(0, t) = 0.1°C$ and conduct two computer experiments. In each experiment, we compare numerically and analytically computed locations of an isotherm corresponding to the temperature T_* such that $\theta(T_*) = 0.999$, that is, 99.9% of water is frozen at $T = T_*$. For the rest of this section, we call T_* the temperature of freezing point depression. In each experiment all parameters are the same, except for the parametrization for the liquid pore water fraction θ. We use either Type A or B water fraction curve in each experiment.

After conducting the numerical both numerical experiments and computing corresponding analytical solutions, we plot all four plots in Figure A1. The displayed curves represent the location of the T_* isotherm in time. Two plots with solid symbols are related to the numerical solutions, while the other two plots with hollow symbols are related to the analytical solutions. The curves marked by rectangles and circles are related to the Types A and B parametrizations, respectively. Note that the difference between the analytical and numerical solutions for each parametrization are negligibly small and the agreement between the related solutions is quite good.

We also emphasize that the thawing line propagates quicker for the Type A parameterization and the difference in time when thawing reaches 0.25 m depth could be different by a factor of two. The latter is primarily due to the fact that the incoming heat flux is primarily absorbed at the region just below the T_* isotherm for the Type A curve and does not significantly penetrate deeper into the soil column. Whereas for the Type B curve, the incoming heat flux penetrates deep into the soil column and produces water phase change at the significant depth.

Acknowledgments
We are grateful to Konstantin Khrulev and Edward Bueler (UAF) for their advice and help with development of the analytical solution. This research was funded by the USGS award G14AP00151, the Next Generation Ecosystem Experiment (NGEE-Arctic) project, the NSF grant ARC-1304271, and by the State of Alaska. NGEE-Arctic is supported by the Office of Biological and Environmental Research in the DOE Office of Science. Support was also provided by the Russian Science Foundation (project RNF 16-17-00102). Numerical calculations for this work were supported in part by the high-performance computing and data storage resources operated by the Research Computing Systems Group at the University of Alaska Fairbanks, Geophysical Institute. The data used are listed in the references and the supporting information. We are thankful to reviewers and the Editor for valuable suggestions making the manuscript easier to read and understand.

References

Anderson, D., & Morgenstern, N. (1973). Physics, chemistry and mechanics of frozen ground: A review. In *Proceedings Second International Conference on Permafrost* (pp. 257-288). Yakutsk, USSR.

Best, M. J., Pryor, M., Clark, D. B., Rooney, G. G., Essery, R. L. H., Menard, C. B., et al. (2011). The Joint UK Land Environment Simulator (JULES), model description - Part 1: Energy and water fluxes. *Geoscientific Model Development*, 4(3), 677-699.

Burn,C.,& Smith,C. (1g88). Observations of the "thermal offset" in near-surface mean annual ground temperatures at several sites near Mayo, Yukon territory,Canada. *Arctic, 4 1*(2), gg_ 104.

Calmels, F, Froese, D., & Clavano, W.(2012). Cryostratigraphic record of permafrost degradation and recovery following historic (18g8-1992) surface disturbances in the Klondike region, central Yukon territory. *Canadian Journal of Earth Sciences, 49(8),* g38-g52. https://doi.org/10.113g/e2012-023

Carslaw,H,& Jaeger,J. (lgsg), *Conduction of heat in solids.* London: Oxford University Press.

Cox, P, Betts, R., Bunton,C.,Essery, R., Rowntree, P,& Smith,J. (1999).The impact of new land surface physics on the GCM simulation of climate and climate sensitivity. *Climate Dynamics, 1S(3),* 183-203.

Froese,D. G.,Westgate,J.A.,Reyes,A.V,Enkin,R.J.,& Preece,S.J.(2008).Ancient permafrost and a future,warmer Arctic. *Science, 321* (58g6), 1648-1648. https://doi.org/10.1126/science.11S7S2S

Goodrich, L. E.(1g78). Some results of a numerical study of ground thermal regimes, *Third lnternational Conference on Permafrost* (Vol. 1,pp. 2g-34). Ottawa:National Research Council.

Gupta, S.(2003). *The classical Stefanproblem.* Amsterdam:Elsevier.

Hobbs,P.(1g74). */ce physics.* Oxford:Claredon Press.

IPCC (2013).In T.F. Stocker,et al. (Eds.), *Climate change 2013: The physical science basis. Contribution of Working Group l to the Fifth Assessment Report of the lntergovemmental Panel on Climate Change* (pp. 1535).Cambridge, UK and New York,USA; Cambridge University Press.

Jaeger,J.C.,& Sass,J.H.(1964). A line source method for measuring the thermal conductivity and diffusivity of cylindrical specimens of rock and other poor conductors. *Joumal of Applied Physics, 1S,* 1187-1194.

James, M, Lewkowicz, A., Smith, S.,& Miceli,C. (2013). Multi-decadal degradation and persistence of permafrost in the Alaska Highway corridor, northwest Canada. *Environmental Research Letters,* 8(4), 045013.

Jorgenson, M.,Romanovsky,V.,Harden,J,Shur, Y.,O'Donnell,J,Schuur,E.,et al. (2010).Resilience and vulnerability of permafrost to climate change. *Canadian Joumal of Forest Research,* 40(7), 121g-1236.

Jorgenson,T.,Yoshikawa,K,Kanevskiy,M.,Shur,Y.,Romanovsky,V.,Marchenko,S,etal.(2008).Permafrost characteristics of alaska. In D.Kane & K.Hinkel (Eds.), *Ninth International Conference on Permafrost, Extended Abstracts* (pp. 121-122).Fairbanks:Institute of Northern Engineering,University of Alaska.

Kaufman, D,Ager,T.A,Anderson, N.J,Anderson,P. M.,Andrews,J.T.,Bartlein,P.T.,et al.(2004).Holocene thermal maximum in the western Arctic (0-180°W). *Quaternary Science Reviews,* 23(5-6), 52g-S60. https://doi.org/10.1016/j.quascirev.2003.09.007

Klute, A.(1g52). A numerical method for solving the flow equation for water in unsaturated materials. *Soil Science,* 73(2), 105-116.

Kress, R. (1998). *Numerical analysis* (pp.344). Germany:Springer.

Kudriavtsev,V,& Melamed,V.(1g72). Asymmetry of the enveloping curves of temperature fluctuations in soil in relation to the calculations of depths of seasonal and perennial freezing. *Permafrost Research, 12,* 3-8.

Lavrushin,Y,& Alekseev, M.(200S). Cenozoic climatic and environmental changes in Russia, Velichko A.A. and V.P.Nechaev (eds), chap.The Arctic regions,Wright Jr., H.E.,T.A.Blyakharchuk,A.A. Velichko and O. Borisova (Eds,English edition),The Geological Society of America, Special Paper 382, 226 p.

Lovell,C. (1g57).Temperature effects on phase composition and strength of partially frozen soil. *Highway Research Board Bulletin, 168,* 74_gs,

Nicolsky,D., Romanovsky,V.,& Panteleev, G.G.(2009). Estimation of soil thermal properties using in-situ temperature measurements in the active layer and permafrost. *Cold Regions Science and Technology, SS,* 120-12g.

Nicolsky,D., Romanovsky,V.,& Tipenko, G.(2007).Using in-situ temperature measurements to estimate saturated soil thermal properties by solving a sequence of optimization problems. *The Cryosphere, 1,* 41-58.

Nixon,J.(1g86).Thermal simulation of subsea permafrost. *Canadian Journal of Earth Sciences, 23,* 203g_2046.

Oleson,K.W,Lawrence, D. M,Bonan,G.B.,Drewniak, B., Huang, M., Koven, C. D,et al.(2013). Technical description of the community land model (CLM) (NCAR tech.note NCAR/TN-503+STR). Boulder,Colorado:NCAR.

Oleson, K, Niu, G.-Y.,Yang,Z.-L., Lawrence, D. M.,Thornton, P.E, Lawrence, P.J., et al. (2008). Improvements to the community land model and their impact on the hydrological cycle. *Journal of Geophysical Research, 1 13,* GO1021.https://doi.org/10.102g/2007JGOOOS63

Osterkamp,T.E.(2003). A thermal history of permafrost in alaska. In M. Phillips,et al. (Eds.), *Proceedings of the 8th International Conference on Permafrost* (Vol.2,pp.863-868).Lisse:Swets & Zeitlinger.

Osterkamp,T.E.,Jorgenson, M.T., Schuur, E.A.G., Shur, Y. L.,Kanevskiy,M. Z.,Vogel,J.G,& Tumskoy,V. E.(2009). Physical and ecological changes associated with warming permafrost and thermokarst in interior alaska. *Permafrost and Periglacial Processes,* 20(3), 235-256. https://doi .org/10.1002/ppp.656

Osterkamp,T.E,& Romanovsky,V.E.(199g),Evidence for warming and thawing of discontinuous permafrost in alaska. *Permafrost and Periglacial Processes, 10,* 17-37.

Osterkamp,T,Zhang,T.,& Romanovsky,V.(1994). Evidence for a cyclic variation of permafrost temperatures in northern alaska. *Permafrost and Periglacial Processes, S,* 137-144.

Philip,J.(1g55). Numerical solution of equations of the diffusion *type* with diffusivity concentration-dependent. *Transaction of the Faraday Society, S1(7),* 88S-8g2.

Renssen, H., Seppa, H,Heiri, O., Roche, D., Goosse, H.,& Fichefet, T.(2009). The spatial and temporal complexity of the Holocene thermal maximum. *Nature Geoscience, 2,* 411-414.

Reyes,A.V,Froese, D.G.,& Jensen,B.J.(2010).Permafrost response to last interglacial warming:field evidence from non-glaciated Yukon and Alaska. *Quaternary Science Reviews,* 29(23-24), 32S6-3274. https://doi.org/10.1016/j.quascirev.2010.07.013

Romanovsky,V., & Osterkamp, T.(1ggs). lnterannual variations of the thermal regime of the active layer and near-surface permafrost in northern Alaska. *Permafrost and Periglacial Processes,* 6, 313-335.

Romanovsky,V.,& Osterkamp,T.(2000).Effects of unfrozen water on heat and mass transport processes in the active layer and permafrost. *Permafrost and Periglacial Processes, 1 1,* 21g-23g,

Romanovsky, V., Smith, S.,& Christiansen, H.(2010).Permafrost thermal state in the polar northern hemisphere during the international polar year 2007-2009: A synthesis. *Permafrost and Periglacial Processes, 21,* 106-116.

Romanovsky, V,Smith, S., Christiansen, H., Shiklomanov, N,Drozdov, D., Oberman, N., et al. (2013). Arctic Report Card 2013, chap. Permafrost,pp. 131-136, NOAA,http://www.arctic.noaa.gov/reportcard

Romanovsky, V., Smith, S.L, Christiansen, H. H., Shiklomanov, N. I., Streletskiy, D. A, Drozdov, D.S., et al.(201SJ. Terrestrial permafrost [in State of the Climate in 2014]. *Bulletin of the American Meteorological Society,* 96(7), S13g-s141.

Romanovsky, V., Yoshikawa, K., Marchenko, S. S., Kholodov, A. L., Muskett, R. R., Alexeev, S.V.,et al.(2010). Thermal state of permafrost in Russia. *Permafrost and Periglacial Processes, 21,* 136-155.

Shur, Y. L., & Jorgenson, M. T. (2007). Patterns of permafrost formation and degradation in relation to climate and ecosystems. *Permafrost and Periglacial Processes*, 18(1), 7-19. https://doi.org/10.1002/ppp.582

Tice, A., Black, P., & Berg, R. (1989). Unfrozen water contents of undisturbed and remolded alaskan silt. *Cold Regions Science and Technology*, 17(2), 103-111. https://doi.org/10.1016/S0165-232X(89)80001-1

Vaughan, D. G., Comiso, J. C., Allison, I., Carrasco, J., Kaser, G., Kwok, R., et al. (2013). Climate change 2013: The physical science basis. In T. F. Stocker, et al. (Eds.), *Contribution of Working Group I ta the Fifth Assessment Report of the Intergovernmental Panel on Climate Change* (Chap. Observations: Cryosphere, pp. 317-382). Cambridge University Press, Cambridge, United Kingdom and New York, NY, USA.

Westermann, S., Langer, M., Boike, J., Heikenfeld, M., Peter, M., Etzelmuller, B., & Krinner, G. (2016). Simulating the thermal regime and thaw processes of ice-rich permafrost ground with the land-surface model cryogrid 3. *Geoscientific Model Development*, 9(2), 523-546.

Williams, P. (1967). Properties and behaviour of freezing soils (Tech. Rep. 72). Norway: Norwegian Geotechnical Institute.

Williams, P. (1982). *The surface of the Earth:* An *introduction to geotechnical science*. London: Longman.

Yoshikawa, K., Bolton, W., Romanovsky, V., Fukuda, M., & Hinzman, L. (2002). Impacts of wildfire on the permafrost in the boreal forests of interior Alaska. *Journal of Geophysical Research*, *107*, 8148. https://doi.org/10.1029/2001JD000438, printed 108(D1), 2003.